Controlled source electromagnetic inversion for resource exploration

Douglas Oldenburg[1], Robert Eso[1], Scott Napier[1], and Eldad Haber[2] discuss their work on inverting controlled source electromagnetic data as a means to enhance the effectiveness of electrical conductivity in exploration for both minerals and hydrocarbons.

Electrical conductivity is a diagnostic physical property for a variety of problems in mineral and hydrocarbon exploration. In mineral exploration, it can sometimes be related directly to the sought mineralization or it can be used to delineate geologic structure associated with the deposit. In oil exploration, conductivity can be a direct hydrocarbon indicator.

One of the main impediments to using electromagnetic (EM) surveys is the complexity of the data. Unlike gravity or magnetic surveys, where the data can sometimes be used to infer geology or possibly to identify drill targets, EM data images are complex and are not connected with geology in a simple way. Over the last few years, however, we have developed computer algorithms to invert controlled source EM (CSEM) data. This opens the door for enhanced applications and for re-assessment of how data are collected and interpreted.

The purpose of this article is to illustrate these ideas by applying our inversion techniques to synthetic and field data relevant to resource exploration. We begin with some background about EM surveys and our forward modelling. In an EM survey, the transmitter, or source, can be a grounded dipole or a loop which carries a time varying current. The measurements can be an electric field (E), a magnetic field (H) or its time derivative (dH/dt).

The governing equations are those of Maxwell and the data are dependent upon three physical properties: electrical conductivity, magnetic permeability, and electrical permittivity. In this article we neglect the effects of electrical permittivity and assume that magnetic permeability is equal to that of free space. We concentrate upon the electrical conductivity, σ (or its reciprocal, resistivity, ρ), which, as illustrated by Table 1, varies by many orders of magnitude in earth rocks and minerals.

EM survey and forward modelling

In frequency domain EM surveys, the transmitter carries a sinusoidal current. The source can be a closed loop or a grounded dipole and data can be measured in the air, on the Earth's surface, or in boreholes. As an example, we consider

Table 1 *Electrical properties of rocks and minerals. (From Applied Geophysics, Telford, W.M., et al., 1976, University Press.).*

Rock Type	Resistivity range (Ωm)
Granite	$3 \times 10^2 - 10^6$
Basalt	$10 - 1.3 \times 10^7$
Sandstones	$1 - 6.4 \times 10^8$
Limestones	$50 - 10^7$
Oil Sands	$4 - 800$
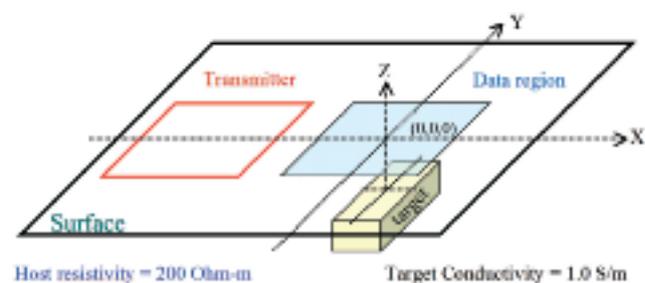
Figure 1 *The transmitter is a 1 km square loop. Measurements are taken over a 1 km square area. The goal is to find the conductive target.*

a typical scenario for a mineral application. Figure 1 shows a large transmitter loop with data collected at the surface in a region outside the loop. The goal is to find the conducting target at depth. To numerically simulate the EM fields, Maxwell's equations are reformulated with the variables being a vector and scalar potential ([1], [2]). A volume, which includes the air and the solid earth, is divided into cells, each of which has a constant conductivity. Finite volume methods are used to discretize Maxwell's equations, along with suitable boundary conditions, on a staggered grid. This results in a large matrix system to be solved, and a solution is obtained using a preconditioned conjugate gradient algorithm. Electric and magnetic fields anywhere in the volume can then be recovered from the potentials.

[1] UBC-Geophysical Inversion Facility, Earth and Ocean Science Department, University of British Columbia, Vancouver, BC, Canada, V6T 1Z4

[2] Department of Mathematics and Computer Science, Emory University Atlanta, GA, 30322.
   E-mail for corresponding author: doug@eos.ubc.ca

Mining Geoscience

When the current in the transmitter is a sinusoid, the resultant electric or magnetic field anywhere in the volume will also be a sinusoid, but it will have an amplitude and a phase that is different from that of the transmitter. The data can be represented as an amplitude and phase, or as real and imaginary parts. The real part is that portion of the signal that is in-phase with the transmitter signal; the imaginary part is that portion that is out-of-phase.

A data map can be generated from a component of the field (e.g. real E_x or imaginary E_y), at a single frequency and from a single transmitter location. For example, a survey that uses six frequencies, measures four fields and has five transmitter locations would generate 120 maps of data. Some selected data maps for the synthetic example in Figure 1 are shown in Figure 2. The information about the conductivity is coded into these various data maps and it is not possible to make geologic inferences by visual interpretation of these images. That goal requires that the data be inverted.

Inversion

The procedure for inverting EM data is identical to that used for other surveys. The inverse problem is cast as an unconstrained optimization problem. An objective function, composed of a misfit term (quantifying how well the observations are being fit) and a model objective function (which incorporates a priori information and causes the solution to have particular structural characteristics) is minimized. A regularization parameter, which controls the relative importance of misfit and structure in the solution, also needs to be determined. In previous articles ([3], [4]) we have elaborated upon the inverse procedure and shown applications of inverting gravity, magnetic, DC resistivity and IP data to recover 3D volumes of the associated physical properties.

For our EM inverse problem we use an iterative Gauss-Newton procedure [5]. Numerical computations are made efficient by writing the large-dense sensitivity matrix as a product of sparse matrices, and by using preconditioned conjugate gradient algorithms for solving the final matrix system of equations.

Synthetic data (E_x, E_y, H_x, H_y, H_z) at six frequencies between .01, and 1000 Hz, generated using the example geometry in Figure 1, were contaminated with noise and subsequently inverted. Figure 3 shows the results displayed in iso-surface format and also pixel elements for a vertical cross-section. The inversion recovers a smoothed version of the conductive block. The predicted data from the inverted model look essentially the same as the observations so they are not plotted here.

The synthetic example provides a synopsis of the inversion and some insight regarding the type of model that will be reproduced from the inversion. We next turn to a field data example.

Geologic background

The Antonio deposit is a high sulfidation gold deposit located in the Peruvian Andes. Gold mineralization of the Antonio deposit is confined to massive silica, vuggy silica, and granular silica alteration [6]. The main alteration control is the intersection of NNE and EW faults. Later structures, striking N45W, crosscut the NNE and EW faults but are post-mineralization. Surface lithologies, structural features and a cross section through the deposit are shown in Figure 4. The outcrop of the deposit is the arc shaped, fault-bounded zone of laminated and brecciated rock.

Geophysical surveys

CSEM and DC resistivity surveys were conducted over the Antonio deposit, with the aim of mapping the high resistivities associated with silicification. Figure 5 shows the location of the geophysical surveys. Two transmitters, each approximately 2 km in length, were used. *E* fields parallel to the transmitter, and *H* fields perpendicular to the transmitter, were acquired. The amplitude of the electric field, measured at 4 Hz, is shown in Figure 6.
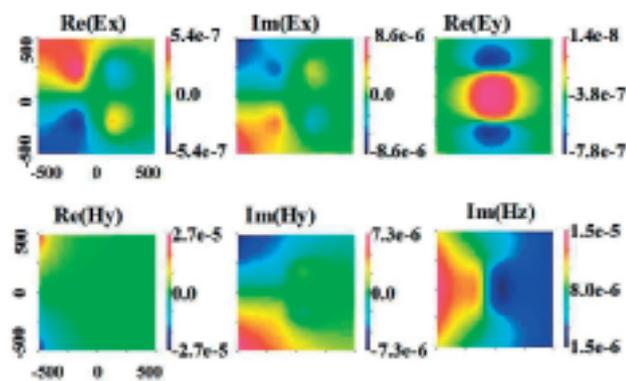

Figure 2 *Simulated data for a transmitter frequency of 10 Hz using the geometry shown in Figure 1.*
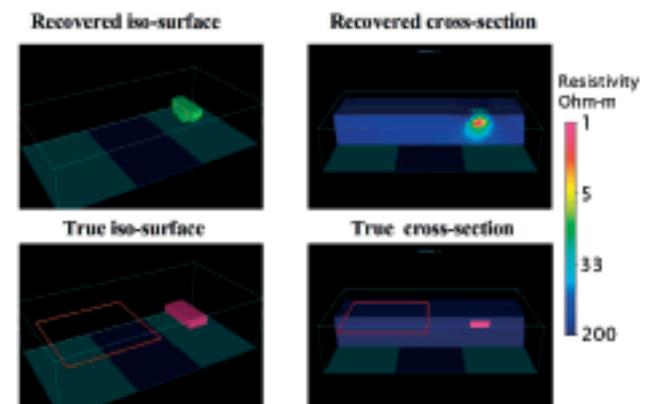

Figure 3 *Comparison of the conductivity model recovered from the inversion (top panels) with the true conductivity (bottom panels).*
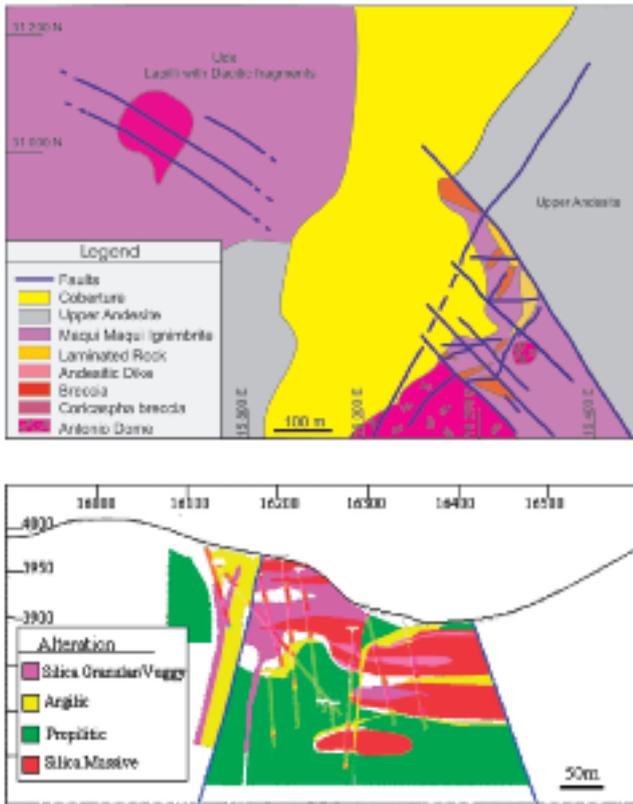
Figure 4 *Surface lithologies (top) and geologic cross section (bottom) of the Antonio deposit, Peru.*
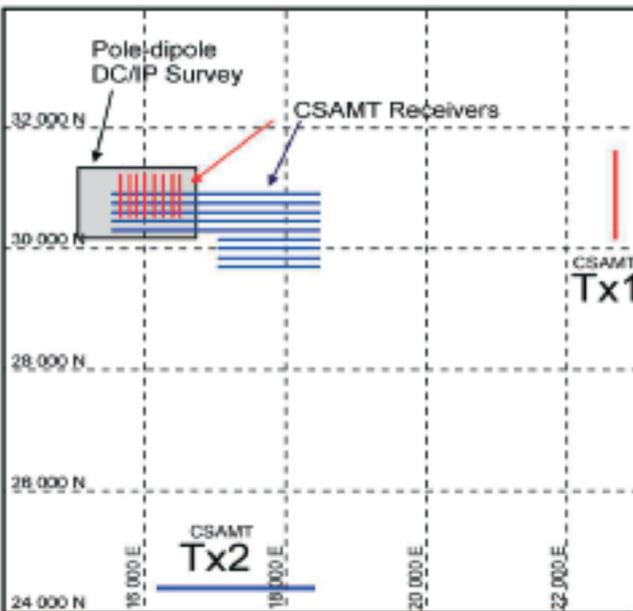

Figure 5 *Antonio geophysical survey map showing the location of CSEM transmitters and receivers and the DC/IP survey area. Airborne time domain EM was flown over the entire region.*

A workflow approach to 3D CSEM inversion

Inverting field data to obtain an informative and high-quality image generally involves a number of steps. Workflows for handling data from different surveys will differ, but there are many elements that are generic to all data sets. Some of these are:

- Understanding the data
- Determining a priori knowledge about conductivity
- Evaluating the importance of topography
- Reducing the size of the problem
- Separately inverting data from each transmitter and frequency
- Simultaneously inverting data from all transmitters and frequencies

We briefly elaborate upon each of these elements as they apply to the Antonio data.

Understanding the data

The location and orientation of the transmitters and receivers, the value of the transmitter current, instrument response functions, and gain factors or normalizations that have been applied to the data must be known so that mathematically modelled responses properly simulate the field data. Unknown normalizations or ad hoc filtering applied to the observations can render them useless for quantitative inversion. Unfortunately, much time is often spent trying to quantify these aspects. Also, if individual fields are to be inverted, then time synchronization between the transmitter and receiver is needed. At Antonio, this was not properly done and hence we were forced to invert impedances $Z = E/H$.

A priori information

The inverse problem is non-unique and the quality of the final result will improve as more information is provided. In particular, an estimate of the background or large-scale conductivity is valuable. The background conductivity serves as a reference model in the inversion and, when well understood, enhances the probability that the recovered model will reflect the earth. It is also needed, as we will show later, for our procedure to reduce the size of the problem. For Antonio CSEM inversion, airborne EM data were inverted to provide an estimate of the conductivity over a region that included
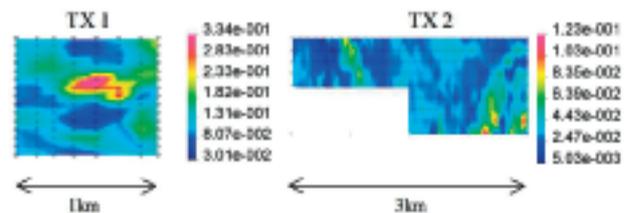

Figure 6 *Amplitude of E-field data from transmitters TX1 and TX2 at 4Hz.*

the area of interest and the transmitters. The simplest representative conductivity was chosen to be a 50 Ω-m half-space.

Assigning errors

It is essential that each datum is accompanied by an estimated uncertainty. This is generally one of the most difficult aspects of an inversion to quantify since the assigned errors ideally should account for additive noise plus any modelling errors such as numerical discretization, mislocation of transmitters, or receivers, etc.

Our procedure was to plot amplitude and phase maps and make a subjective decision about the amplitude of the observed data variations that we wanted to model. This resulted in an error estimate of 5% for the amplitude of the impedances and 2° for the phase.

Assessing the effects of topography

Surface topography can have a substantial effect on the data. The topography for Antonio, provided in Figure 7, shows that there is nearly a kilometre of vertical relief in the region surrounding the transmitters and data. A comparison between data forward modelled with and without topography showed that it was essential to include topography in the numerical modelling.

Reducing the size of the problem

The size of the cells used in the numerical modelling should be small enough to capture the geologic structure of importance and also be small compared to the skin depth at any frequency. At the same time, the volume that is discretized must be large enough to include the transmitters and the area where data were collected, and also extend to sufficient distances in all three spatial directions so that applied boundary conditions are valid.

Often, attempts to simultaneously satisfy these two goals result in a numerical problem that is excessively large. For instance, in the case of Antonio, the discretized volume
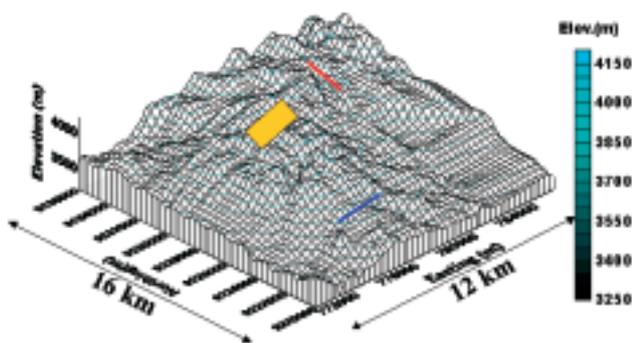
needed to calculated the fields is about 28 x 28 x 4 km (see Figure 5). However, capturing the important geology requires cell sizes that are 25-50 m. To work at this scale, and to make the problem numerically tractable, we first forward model the fields in the large volume using 250 m cells using the conductivity found from the a priori information. Next, a smaller volume around the area of interest is selected and discretized with 50 m cells. The inverse problem on the smaller volume problem is solved subject to the condition that the fields on the boundary are the background fields generated from the large scale modelling. The success of this approach depends upon having a reasonably good estimate of the background conductivity and knowledge of the surrounding topography. The meshes showing the procedure of reducing the volume are shown in Figure 8.

Inverting each frequency individually

It is good practice to invert each frequency individually for each transmitter. This can illuminate particular problems associated with assignment of uncertainties, data normalizations, data quality and effects of discretization. These individual inversions were carried out for Antonio.

Multiple frequency/transmitter inversion for CSEM data

Impedances for each transmitter at frequencies of 4, 64 and 256 Hz were inverted. The combined 3D CSEM inversion result required 1.5 days using a 3.0 Ghz desktop computer and the resultant conductivity model is shown in Figure 9. The observed and predicted data show that the resulting model of electrical conductivity adequately reproduces the observed fields.

The inversion shows a large resistive body, which extends to a depth of approximately 150 m below the surface. This
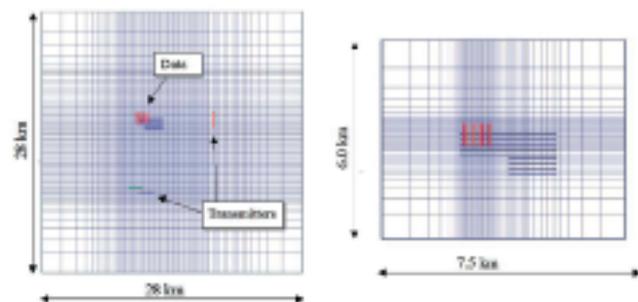
Figure 8 *Discretization for the Antonio CSEM inversions. On the left is the mesh required to encompass the transmitters and survey area. The 28x28 km area requires 236,250 cells for cells with horizontal dimension 250x250 m. The plot on the right shows a discretization of the central region of interest. This smaller volume was 7.5x6.5 km and required 73,226 cells of horizontal size 50x50 m.*
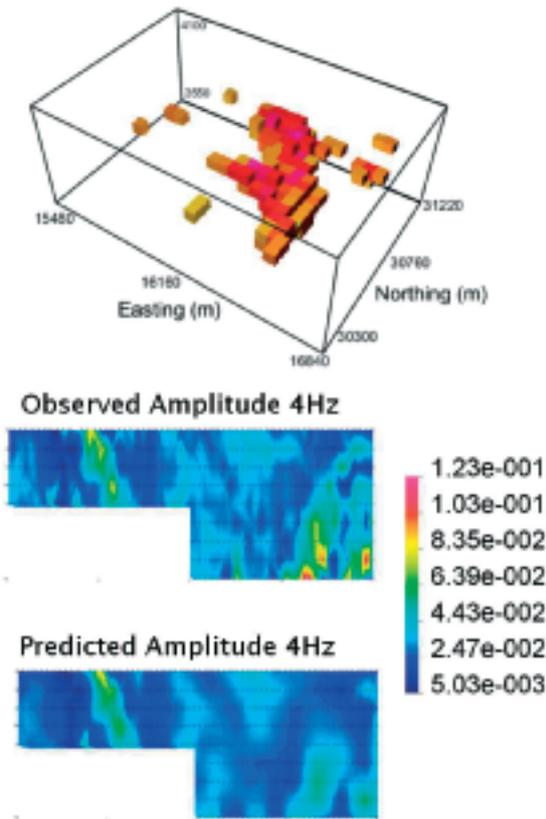

Figure 7 *Topography of Antonio and surrounding region. The transmitter locations are the coloured lines and the area of data collection is the yellow patch.*

Figure 9 *3D CSEM inverted volume using 4, 64, 256Hz from two transmitters. Observed and predicted impedance amplitudes for a single transmitter at 4Hz are shown.*

Figure 10 *3D DC resistivity inverted volume with the corresponding observed and predicted pole-dipole data plotted as apparent resistivity.*

resistive target is attributed to silicification, and is associated with gold mineralization. The 3D inversion model agrees with surface lithologies observed at the Antonio site and with drilling results.

3D DC resistivity inversion

Pole-dipole DC resistivity data were also collected over the Antonio deposit (Figure 5). The survey consisted of four lines, each separated by 150 m and a station spacing of 50 m. The data were inverted using the same inversion procedure as the CSEM, but with a different algorithm that involved computing only the scalar electric potential. The volume for inversion consisted of 35, 910 cells, with the smallest cell size being 25 x 25 x 12.5 m. The resulting image of electrical resistivity is shown in Figure 10, along with the observed and predicted data.

The inversion result shows a large resistive body mapping quartz mineralization. The shape, size and location of the body is very similar to that obtained through the CSEM inversion. We note that the resulting volumes derived using 3D CSEM and 3D DC resistivity inversions, shown in Figures 9 and 10, are plotted on the same colour scale and use the same cut-off value for the iso-surface. A more detailed comparison
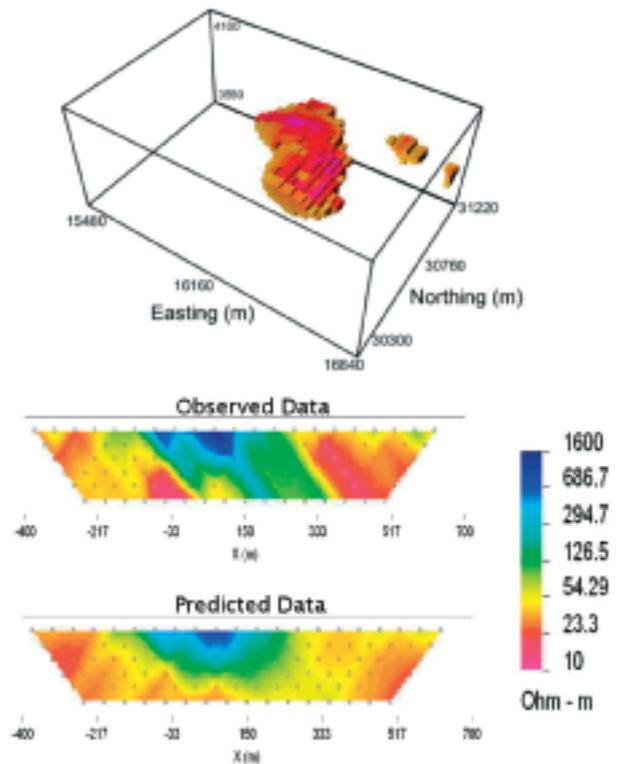
of the CSEM and DC resistivity inversions is shown in Figure 11. Cross sections and plan view maps of the two resulting models are plotted side-by-side. Fault structures are overlain on these plots, showing that the silicification is bounded between two near vertical faults, which are the NNE trending faults seen in Figure 4.

The general agreement between the recovered resistivities from two independent geophysical survey techniques is very encouraging. It provides additional confidence that the major features shown in those figures are representative of the true resistivity.

Seafloor EM surveys

CSEM surveys also have an application in marine hydrocarbon exploration. Water-filled marine sediments are quite conductive at roughly 1–5Ω-m while hydrocarbon-filled reservoirs are thought to be at least an order of magnitude more resistive. Thus determining if a potential prospect is resistive can provide complementary information to seismic interpretation and reduce the risk of drilling an unproductive well. For a hydrocarbon reservoir, the EM target is a resistor which is typically very thin compared to its horizontal extent. While a reservoir may extend for several kilometres in the lateral directions, it may be only 10 to 100 m thick.
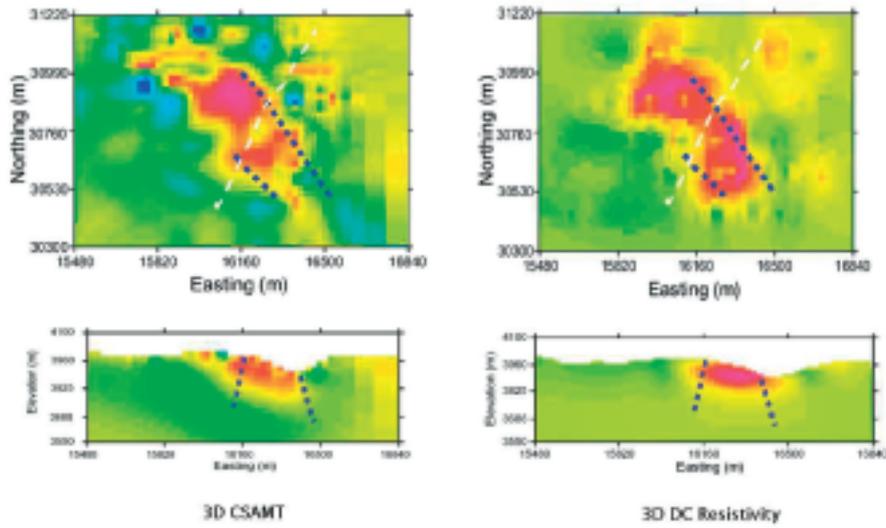
Figure 11 *3D CSAMT and 3D DC resistivity inversion cross section and plan view sections. Both plan view sections are at a depth of 3900 m.*

The reservoir might also be buried a kilometre or more beneath the ocean floor which is itself hundreds of metres, or kilometres, beneath the sea surface.

The geophysical survey consists of deploying electric and magnetic field sensors on the ocean floor and towing an electric dipole source along lines over the area of interest. Current flowing in the earth is channelled away from the resistor and this causes distortions of the EM fields. The frequency of the sinusoidal current in the transmitter is typically 0.1–10 Hz and hence penetration depths can extend to several kilometres. The survey is sometimes referred to as seabed logging. [7] [8] To help illustrate the potential of marine CSEM surveys for hydrocarbon exploration, we apply our forward modelling and inversion to a synthetic problem.

A reservoir model is shown in Figure 12. Data were generated for 1 and 5 Hz and for nine receivers along two orthogonal lines. The transmitters lie on a series of east-west lines 500 m apart. The E_x data for a single receiver are shown in Figure 13. The inversion was performed using the same code as for the mineral exploration example. A sample comparison of the observed and predicted data is found in Figure 13. Figure 14 shows the recovered model from the inversion plotted as pixel values and as an iso-surface. There are some moderately conductive artifacts above and below the target, but overall the reservoir shape and conductivity is well recovered.

Figure 14 shows that inversion of seafloor EM data has the potential to recover reservoir geometry and a good estimate of resistivity. Even better information might be obtainable if EM data were inverted along with some constraints imposed by an interpretation of seismic data. This is clearly a situation where seismic and EM data can provide complementary information.

Summary comments

In this article we have attempted to illustrate the practical capabilities of inverting frequency domain EM data for exploration problems. The ability to invert data means that we are no longer restricted to acquiring data that can only be interpreted through data plots or with algorithms that require simplifying assumptions, such as being in the far-field of the transmitter. This opens the door for research on more cost-effective survey design. In particular, the transmitters in typical CSAMT surveys can be brought closer to the area of interest and thereby increase the signal-to-noise ratio and reduce acquisition costs. Also, individual fields can be inverted. The advantages of doing this need to be thoroughly inves-
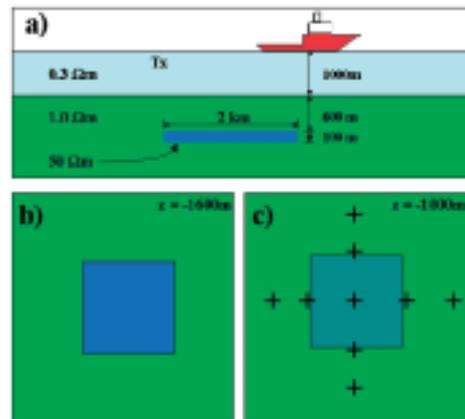

Figure 12 *Profile and planview sections for a synthetic model for a marine CSEM survey are shown respectively in (a) and (b). A 2 km x 2 km x 100 m reservoir of 50 Ω-m is buried in a background of 1 Ω-m. The sea water is 0.3 Ω-m. The pattern of receiver locations on the seafloor is shown by the crosses. The resistive target has a footprint shown in blue.*
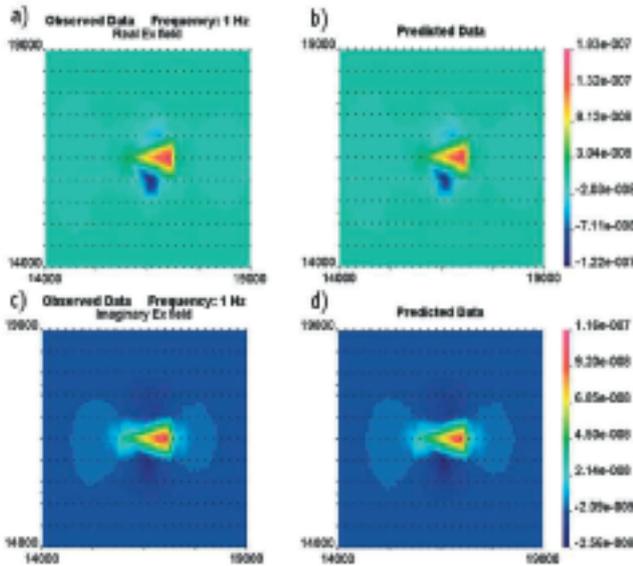
Figure 13 *Forward modelled (Observed) data for the Ex component of a single receiver at 1 Hz are shown in panels (a) and (c). Dots show transmitter locations on East-West lines. The predicted data from the inverted model are shown in panels (b) and (d).*
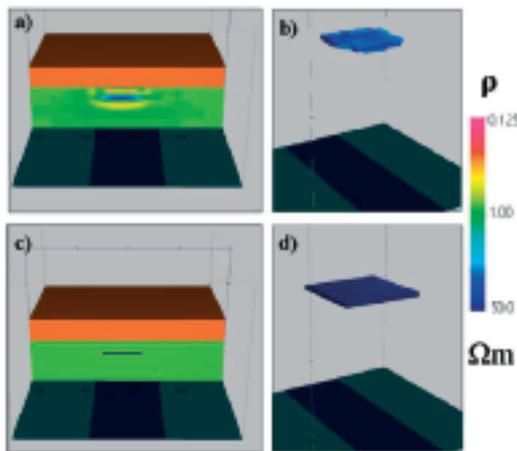

Figure 14 *Cross-sections of the recovered and true models are shown in (a) and (c) respectively. Iso-surface representations are shown in (b) and (d).*

tigated but, in principle, there should be more information in the two individual fields E and H than in their ratio.

Modern surveys that collect these individual fields need to keep track of any normalizations so that the data can be properly modelled. Irrespective of whether we are working in a minerals application or are involved in a marine EM survey for hydrocarbons, our analysis shows that acquiring multi-components of fields at many locations and at a few frequencies can yield a great deal of 3D information. We also know that depth of investigation, and the amount of struc-

ture obtained in an inversion, is quite dependent upon the signal/noise level of the data. Combining these two statements leads to the hypothesis that acquiring high quality data at a few well chosen frequencies may be more effective than acquiring noisier data at many frequencies.

Finally, we emphasize that 3D inversion of EM data in all realistic exploration problems is a non-trivial task and that there are many places at which the inversion can get derailed. High quality results can be obtained only through implementation of a well-designed workflow and through interaction between geoscientists who are knowledgeable about the area of interest and the exploration goals.

Acknowledgements

References

[1] Haber, E., Ascher, U., Aruliah, D., and Oldenburg, D. [2000] Fast modelling of 3D electromagnetic problems using potentials, *J. of Comp. Phys.*, **163**, 150-171.

[2] Haber, E. and Ascher, U. [2001] Fast finite volume simulation of 3D electromagnetic problems with highly discontinuous coefficients. *SIAM J. Scient. Comput.*, **22**, 1943-1961.

[3] Phillips, N., Oldenburg, D., Chen, J., Li, Y., and Routh, P. [2001] Cost effectiveness of geophysical inversions in mineral exploration: Applications at San Nicolas. *The Leading Edge*, **20**, 12, 1351.

[4] Oldenburg D.W., Li Y., Farquharson C.G., Kowalczyk P., Aravanis T., King A., Zhang P., and Watts A. [1998] Applications of Geophysical Inversions in Mineral Exploration Problems. *The Leading Edge*, **17**, 461- 465.

[5] Haber, E., Ascher, U., and Oldenburg, D. [2004] Inversion of 3D electromagnetic data in frequency and time domain using an inexact all-at-once approach. *Geophysics*, **69**, 1216-1228.

[6] Oldenburg, D., Shehktman, R., Eso, R., Farquharson, C.G., Eaton, P., Anderson, B., and Bolin, B. [2004] Closing the gap between research and practice in EM data interpretation. *SEG Technical Program Expanded Abstracts*, 1179-1182.

[7] Ellingsrud, S., Eidesmo, T., Johansen, S., Sinha, M.C., MacGregor, L.M., and Constable, S. [2002] Remote sensing of hydrocarbon layers by seabed logging (SBL): Results from a cruise offshore Angola. *The Leading Edge*, **21**, 10, 972-982.

[8] Johansen, S., Amundsen, H.E.F., Rsten, T., and Ellingsrud, S. [2005] Subsurface hydrocarbons detected by electromagnetic sounding. *First Break*, **23**, 3, 31-36